

# Single-grain and multi-grain OSL dating of river terrace sediments in the Tabernas Basin, SE Spain

**Geach, M.R. ; Thomsen, Kristina Jørkov; Buylaert, Jan-Pieter; Murray, Andrew; Mather, A.E. ; Telfer, M.W. ; Stokes, M.**

*Published in:*
Quaternary Geochronology

*Link to article, DOI:*
10.1016/j.quageo.2015.05.021

*Publication date:*
2015

*Document Version*
Peer reviewed version

# Single-grain and multi-grain OSL dating of river terrace sediments in the Tabernas Basin, SE Spain

Geach, M.R.[1,*], Thomsen, K.J.[2], Buylaert, J.-P.[2,3], Murray, A.S.[3], Mather, A.E.[1], Telfer, M.W[1]., Stokes, M[1]

[1] School of Geography, Earth and Environmental Sciences, Plymouth University, Drakes Circus, Devon PL4 8AA, UK

[2] Center for Nuclear Technologies, Technical University of Denmark, DTU Risø Campus, Denmark.

[3] Nordic Laboratory for Luminescence Dating, Department of Geoscience, University of Aarhus, Risø Campus, Denmark

* Corresponding author: martin.geach@plymouth.ac.uk

## Abstract

River terraces represent important records of landscape response to forcing mechanisms (e.g. tectonic uplift and climatically driven changes in sediment availability) in the Iberian Peninsula. In this study, Optically Stimulated Luminescence (OSL) dating was used to date sediments in two principal river terraces in the Tabernas Basin, SE Spain. A total of 23 samples were collected from the fluvial terraces for dating using quartz OSL. Sixteen of the samples could not be dated because of low saturation levels (e.g. typical $2xD_0$ < 50 Gy). The remaining seven samples (5 fossil and 2 modern analogues) were investigated using both multi-grain and single-grain analysis. Single grain results show that: (i) measurements from multi-grain aliquots overestimate ages by up to ~ 4 ka for modern analogues and young samples (< 5 ka), and (ii) that the presence of many saturated grains has biased the multi-grain results to older ages. Despite the unfavourable luminescence characteristics we are able to present the first numerical ages for two terrace aggradation stages in the Tabernas Basin, one at ~16 ka and the other during the Mid-Late Holocene.

# 1 Introduction

In the Tabernas Basin southeast Spain, river terraces record the effects of basin-wide aggradational and incisional events, as driven by external and internal forcing agents (e.g. tectonics, climate and lithological controls) throughout the Quaternary (Harvey et al., 2003; Nash and Smith; 2003). The basin is one of a series of interconnected Neogene sedimentary basins located within the Internal Zone of the Betic Cordillera (Betics) (Fig. S1A). The Quaternary basin morphology records considerable variation in vertical incision over a lateral distance of ~12 km (Fig. S1B). In the east of the basin, the landscape is dominated by aggradational alluvial fans that record little incision (< 10 m). In contrast, the central and western parts of the basin record up to 250 m of incision (i.e. vertical separation of current river bed and the uppermost Quaternary terrace surface), with the formation of a sequence of inset fluvial terraces (i.e. a river terrace staircase). The variation in basin incision is typically attributed to regional differences in tectonically-driven base-level change (Harvey, 2007). However, Harvey et al. (2003) and Alexander et al., (2008) suggest that climatic factors and further internal controls (e.g. variations in lithological strength) are also of significance in the delivery and routing of sediment both to, and within, the basin.

Unfortunately, due to the poor preservation of organic materials in the terrace record and the lack of application of other dating methods (e.g. luminescence, cosmogenic nuclide dating), little is known concerning the timing of major periods of landscape change in the basin (Nogueras et al., 2000). In this study, we use quartz optically stimulated luminescence (OSL) to date fluvial samples obtained from two terrace levels in the Tabernas Basin. Quartz OSL was selected for investigation because of the ubiquity of quartz, and because quartz OSL is reset rapidly on exposure to daylight (e.g. Jain et al., 2004a). One of the key assumptions in OSL dating is that the signal was adequately reset at deposition, so that any residual signal is insignificant compared to the burial signal. If this is not the case, an OSL age based on standard multi-grain aliquots is likely to overestimate the depositional age, because of the presence of poorly-bleached grains.

One approach to identifying the potential for significant incomplete bleaching is to make use of the differential bleaching rates of quartz and feldspar luminescence signals; these signals bleach at very different rates (about one order of magnitude difference) and so by comparing quartz OSL and feldspar (post-IR) IRSL ages, it should be possible to determine whether a given quartz sample is likely to have been well-bleached at deposition (e.g. Murray et al., 2012). This approach of course requires the presence of suitable feldspar grains, which are not always common in mature sediments.

Another approach to identifying the likelihood of significant incomplete bleaching is to measure the doses recorded by very young or modern sediments (modern analogues; e.g. Murray and Olley, 2002; Jain et al., 2004a; Vandenberghe et al., 2007; Porat et al.,2010; Murray et al., 2012). Here the assumption is that the recent sedimentary environment is analogous to that of the fossil samples, although such modern analogues are likely to be worst-case scenarios due to a low preservation potential (Jain et al., 2004a). The average multi-grain residual dose from young or modern quartz samples from fluvial and colluvial environments around the world is ~2 Gy (67 samples; Murray et al., 2012) indicating that in such environments incomplete bleaching is likely only to be of concern in relatively young samples (e.g. < 20 ka).

A third approach in identifying the likelihood of significant incomplete bleaching is to examine the characteristics of single-grain dose distributions, e.g. over-dispersion (OD; Galbraith et al., 1999) and skewness (Bailey and Arnold, 2006). However, Thomsen et al. (2012) have shown that over-dispersion is not a reliable indicator of incomplete bleaching, and Medialdea et al. (2014) found the decision tree model of Bailey and Arnold (2006) resulted in gross underestimations in six out of eight cases. In multi-grain dose distributions, incomplete bleaching is masked by averaging effects (depending on aliquot size and grain sensitivity), but if some of the grains were well-bleached at burial it is possible to identify these by analysing single-grain dose distributions using one of various minimum age models (e.g. review by Duller, 2008) and thus estimate the depositional age accurately.

The principal aim of this study is to use single grain and multigrain OSL techniques in order develop a framework chronology for the youngest river terrace levels in the Tabernas Basin. Here we present both multi-grain and single-grain quartz OSL ages of five fossil and two modern samples from a region with unfavourable OSL characteristics. This dataset provides a valuable basis for the development and application of OSL techniques to the Tabernas Basin and other similar regions in southern Iberia.

## 2 Samples and context

Four levels of Quaternary inset terraces were identified as common across the Tabernas Basin (Fig. 1A; Geach et al., 2014). These occur at ~ 80 m (level 1: oldest), ~ 50 m (level 2), ~ 30 m - 10 m (level 3) and < 5 m (level 4: youngest) above the current channel (Fig. 1B). The sedimentology of the terraces indicates deposition in laterally-extensive alluvial fans for terrace levels 1 and 2 with a later shift to more confined, braided fluvial styles for levels 3 and 4.

Sampling for OSL dating was limited due to the highly indurated nature and coarse grain size (gravel dominated) of most exposures. A total of 23 samples were collected from the fluvial staircase, including two modern analogue samples. No samples were collected from terrace level 1 due to the hazardous location of outcrops. A summary of the sample locations, depths, positions on terrace etc. is presented in Table S1 and sites marked on Fig. 1A. Preliminary studies into the mineralogy of the terrace samples (i.e. XRF analysis of samples) indicated an almost complete absence of potassium feldspar grains and hence focus was placed on the use of quartz OSL.

# 3 Experimental details

Two samples (Tab-5 and Tab-16) were too coarse to provide sufficient medium sand for dating. The remaining 21 samples were sieved (180-250 μm) and processed using standard techniques (HCl, $H_2O_2$,heavy liquids and HF) under subdued red/orange light, to give quartz-rich extracts.

## 3.1 Instrumentation

Multi-grain aliquots (Ø=8 mm, 1000s of grains) were prepared by mounting grains in a single layer in stainless steel cups using silicone oil. Measurements used TL/OSL DA-20 Risø TL/OSL readers with blue light stimulation (λ = 470 nm, ~80 mW/cm$^2$) and photon detection through 7.5-mm of Hoya U-340 glass filter (Bøtter-Jensen et al., 2010). Any measurements above 200 °C were conducted in a nitrogen atmosphere.

Single-grain measurements were carried out using an automated TL/OSL DA-20 Risø reader fitted with a single-grain laser attachment (Bøtter-Jensen et al., 2003). The stimulation light source is a 10 mW solid-state diode-pumped laser emitting at 532 nm; this is focused to a spot < 20 μm in diameter at the sample grain position. Grains were loaded into sample discs each with 100 holes of 300 μm diameter on a 10×10 grid with 600 μm spacing between hole centres. Visual inspection under red light confirmed that a maximum of one grain was loaded into each hole.

## 3.2 OSL measurements

The single-aliquot regenerative-dose (SAR) procedure (Murray and Wintle, 2000) was used for equivalent dose determination, with a minimum of 5 regeneration cycles including a recycling and recuperation measurement. For both multi-grain (blue stimulation for 40 s at 125 °C) and single-grain (green stimulation for 1 s at 125 °C) measurements blue/green stimulation was preceded by IR stimulation at 125 °C for 40 s to minimise contributions from any feldspar signals (Banerjee et al., 2001). Preheats were set at 260 °C for 10 s and cut

heats at 220 °C based on the results of preheat plateau measurements using sample Tab-11 (see Fig. 2A). For multi-grain measurements the signal was summed over the initial 0.6 s of stimulation less a background from the following 1.6 s of stimulation. For single-grain measurements the signal was summed over the initial 0.06 s and the background was derived from the sum over the final 0.15 s. This is because, in contrast to multi-grain stimulation curves, the decay rates of single grain laser-stimulated curves appear to be dominated by variations in effective stimulation power, rather than in the relative intensity of the various OSL components (Thomsen et al., 2015).

All dose response curves (DRC) were fitted using a saturating exponential function of the form $L_x/T_x = I_0*(1-\exp(-D/D_0)$, where $L_x/T_x$ is the sensitivity corrected OSL response, and $I_0$ and $D_0$ are constants. Equivalent dose estimates were derived by interpolation of the sensitivity corrected natural signal onto individual DRCs using Analyst (Duller, 2007). Uncertainties are assigned to individual dose estimates assuming Poisson statistics and include curve fitting uncertainties (Duller, 2007).

### 3.3 Rejection criteria

Initially, standard rejection criteria were applied. For the multi-grain data, aliquots were accepted if the recycling ratio was within 15% of unity. For the single-grain data individual single-grain dose estimates were only accepted if (i) the uncertainty on the test dose response from the natural SAR cycle is less than 30% ($\sigma_{Tn}$<30%), (ii) the recycling ratio was within 2 standard deviations of unity, (iii) the OSL IR depletion ratio (Duller, 2003) was within 2 standard deviations of unity, and (iv) the recuperation is $\leq$1 Gy. We use an absolute recuperation rejection criterion (instead of a commonly used relative recuperation value) to avoid biasing the measured dose distribution by preferentially removing low dose estimates. Furthermore, only grains for which the sensitivity corrected natural signal ($L_n/T_n$) is not in saturation on the DRC (i.e. $L_n/T_n+\sigma_{Ln/Tn}< I_0$, where $\sigma_{Ln/Tn}$ is the uncertainty assigned to $L_n/T_n$), were accepted. The relative number of grains rejected due to saturation is given in Table 1.

## 4 Dosimetry

Radionuclide concentrations were measured using laboratory high-resolution gamma spectrometry. In the laboratory, radionuclide concentrations were measured on homogenised materials collected from the immediate area surrounding the sampling locations. Approximately 200 g of material from each sample location was dried and ignited at 450°C for 24 h to remove any organic matter. The samples were then pulverised and homogenised before mixing with wax and casting in a fixed geometry; this process prevents

loss of $^{222}$Rn and provides a reproducible counting geometry. The samples were stored for at least three weeks to enable $^{222}$Rn to reach equilibrium with its parent isotope $^{226}$Ra. Radionuclide concentrations ($^{238}$U, $^{226}$Ra $^{232}$Th and $^{40}$K) were measured on a high-purity germanium detector for at least 24 hours (Murray et al., 1987). Final dose rates were derived using the conversion factors of Guérin et al. (2011) with calculations of cosmic radiation contributions based on Prescott and Hutton (1995). Saturated water contents were derived from bulk samples for all samples and the life-time average water content was taken to be 20% of saturation. A summary of radionuclide concentrations, assumed moisture content and total quartz dose rates for the samples dated is given in Table 2.

# 5 Luminescence characteristics

## 5.1 Multi-grain OSL characteristics

Multi-grain SAR OSL measurements were undertaken on all samples. During preliminary measurements 16 samples were discarded due to low saturation levels (e.g. typical $2*D_0 <$ 50 Gy; see Table S1 for discarded samples). The OSL signals of the five remaining terrace samples (Tab-9, Tab-10, Tab-11, Tab-20 and Tab-21) and two modern analogue samples (MA1 and MA2) were all dominated by the fast component. Fig. 2B shows a representative DRC from sample Tab-9 and the inset shows a typical OSL curve. Individual sample average recycling ratios were within 5% of unity (mean 1.012±0.014, n=7 samples) and recuperation values were on average less than 1% of the equivalent dose. Multi-grain dose recovery tests (Murray, 1996) were satisfactory for all fossil samples (see inset to Fig. 2C), giving an average dose recovery ratio of 0.97±0.02 (n=46, Fig. 2C) indicating that our SAR protocol can accurately measure a laboratory dose absorbed before any thermal pre-treatment.

## 5.2 Multi-grain dose determination

Multi-grain aliquots consist of many individual OSL-sensitive grains and due to averaging effects any information about e.g. post-depositional mixing or incomplete bleaching is lost (e.g. Olley et al., 1999; Wallinga, 2002). The only meaningful information that can be retrieved from large multi-grain dose distributions is the average dose – either unweighted, or weighted (e.g. using the Central Age Model, CAM; Galbraith et al., 1999) according to the uncertainties assigned to individual dose. The individual multi-grain unweighted (arithmetic) averages and CAM averages are all consistent within 1 standard deviation (data not shown). The relative over-dispersions (OD, Galbraith et al., 1999) range between 13±4 and 51±9 % and, as expected, are completely consistent with the relative standard deviations, i.e. the contribution from counting statistics and curve fitting errors to the relative standard deviation

is not detectable. Thus, for multi-grain dose distributions there appears to be no advantage in deriving CAM dose estimates in preference to an average (arithmetic) dose. The equivalent multi-grain doses given in Table 1 are arithmetic average doses.

## 5.3 Single-grain OSL characteristics

Single grain measurements show that 98% of the measured grains were rejected because the first (natural) test dose response was undetectable (for test doses of 15 Gy), i.e. $\sigma_{Tn}$>30%; the remaining grains were all relatively dim - the median of the first test dose response in the summation period (first 0.06 s) was only ~1.5 counts/Gy/0.06 s. Applying the remaining single-grain rejection criteria, given in section 3.3, resulted in a further reduction in the accepted grain populations by ~20%. However, neither the dose (unweighted arithmetic mean or CAM) nor the relative over-dispersion (OD, Galbraith et al., 1999) changed significantly as a consequence of applying the rejection criteria to the natural and dose recovery dose distributions, i.e. the average ratio of the CAM dose of the dose distribution obtained by using all the rejection criteria and that obtained by only using the $\sigma_{Tn}$<30% criterion is 1.04±0.04 (n=5 samples). The corresponding ratio for the OD is 1.08±0.08. Thus, it would appear that there is no advantage in applying these standard single-grain rejection criteria for these samples, but there is a cost – the rejection of a 20% of otherwise acceptable grains. Similar conclusions have been made by other authors (e.g. Thomsen et al., 2012; Guérin et al., 2015a; Thomsen et al., submitted; Kristensen et al., 2015) for different samples of different origins. Here, we have chosen only to apply the rejection criteria $\sigma_{Tn}$<30% and $L_n/T_n+\sigma_{Ln/Tn}< I_0$.

## 5.4 Single-grain dose estimation

A single grain is the smallest unit of transport and thus it is generally assumed that information about e.g. post-depositional mixing and incomplete bleaching can be extracted from single-grain dose distributions (e.g. Olley et al., 1999; Roberts et al., 2000). It is well-documented that the OSL sensitivity of grains emitting detectable OSL in the response to a laboratory dose varies significantly from one grain to another and typically by several orders of magnitude (e.g. Duller, 2008 and references therein). Thus, the uncertainty assigned to individual dose estimates will also very considerably and it would seem prudent to weight according to individual uncertainties, although it has been argued that the unweighted arithmetic mean dose may provide a more accurate estimation of age, because the average dose rate is used in age calculations (Guérin et al., 2015b).

In Table 1 and 3 we present single-grain equivalent doses calculated using both the unweighted (arithmetic) mean, CAM, CAM un-logged ($CAM_{UL}$; Arnold et al., 2009) and robust statistics (Tukey, 1977). For single-grain dose distributions containing only positive

dose estimates CAM is usually the preferred dose estimation model, because it has been argued that CAM is better suited to the statistical properties of such datasets, particularly for older samples (e.g. Arnold el al., 2009). However, the log normal assumption of the CAM prevents the application of this model to the single-grain dose distributions obtained for several samples in this study (MA1, MA2, Tab-9 and Tab-20), which contain non-positive dose estimates (see Fig. 3). Thus, for these samples we cannot apply the CAM without arbitrary rejection of the non-positive dose estimates. Such arbitrary rejection is not required when using the $CAM_{UL}$ or the arithmetic mean. The latter is not widely reported in single-grain studies; mainly because this average can be biased by outlying, poorly known dose estimates. One approach to minimize the effects of outliers is to apply robust statistics to the data sets before calculation of the arithmetic average. Here, we have arbitrarily but non-subjectively removed outliers identified to be those outside the 1.5×IQR (InterQuartile Range), where IQR is the difference in dose between the highest and lowest dose value of the middle 50% dose values. This approach is the same as that used successfully by Medialdea et al. (2014) for young flash-flood deposits from southeast Spain.

## 5.5 Single-grain dose recovery and $D_0$ criterion

Single-grain beta dose recovery tests were undertaken on sample Tab-9 (given dose 15 Gy) and Tab-21 (given doses of either 40 or 60 Gy) and the results are summarised in Table S2. The dose recovery dose distributions are given in Fig. S2. The dose distribution for the 40 Gy experiment contains a single non-positive dose estimate of -5±16 Gy and the CAM values reported for this experiment have been obtained by the arbitrary rejection of this dose estimate. The CAM dose recovery ratios (i.e. measured dose calculated using CAM) for these samples are 1.02±0.04 (n=83; 15 Gy Tab-9), 0.93±0.07 (n=35; 40 Gy Tab-21) and 0.76±0.08 (n=45; 60 Gy Tab-21) with corresponding relative ODs of 15±5%, 27±6% and 59±8% (see Table S2). The average CAM dose recovery ratio is 0.90±0.08 (n=3). The number of grains rejected due to saturation range between 5 and 14%. These results indicate that our ability to recover a known laboratory dose accurately appears to decrease with increasing dose.

All these experiments contained grains for which the natural sensitivity corrected signal was in or above saturation of the laboratory dose response and thus no dose estimate could be calculated for these grains (see Table S2). The presence of such grains is a cause for concern as their removal is very likely to involve bias to lower doses. Thomsen et al. (submitted) suggested an alternative rejection criterion which seems to provide an unbiased approach (i.e. independent of the absolute value of individual dose estimates) to the non-

subjective rejection of saturated grains (or grains close to saturation). In this approach the individual $D_0$ values of all grains are determined and only those dose estimates from grains with a $D_0$ value equal to or greater than a certain threshold (or cut-off) value, *x*, are accepted; this threshold value *x* is selected to be the same as the average equivalent dose calculated when the rejection criterion is employed. This requires iteration; the threshold value *x* is determined by calculating the average (weighted or unweighted) dose of the dose distribution as a function of *x*. Thomsen et al. (submitted) found that when the threshold value *x* is equal to the average dose of the sample the otherwise unacceptably low dose recovery ratios became acceptable; i.e. for an average sample dose of 60 Gy only grains with a $D_0$ value larger than 60 Gy are accepted into the initial dose distribution. Then a revised average is calculated and a new threshold set equal to this revised average. This process is repeated until the revised average is equal to or less than the selected threshold. By applying this rejection criterion, both Thomsen et al. (submitted) and Guérin et al. (2015a) obtained dose recovery single-grain dose distributions with acceptable CAM dose recovery ratios. In effect, this process rejects those grains for which the DRC saturates at such a low dose that it is unable to record the dose of interest. It is important to note that setting the threshold value too high does not bias the average dose to higher or lower values. It simply increases the random fluctuation in the average value because of the smaller number of accepted grains.

If we now apply the additional rejection criterion to the $D_0$ values of individual DRCs, then the average CAM dose recovery ratio increases to 0.97±0.03, the dose recovery ratio at 60 Gy is indistinguishable from unity (i.e. from 0.76±0.08 to 0.94±0.08) and the number of grains rejected due to saturation reduces to between 0 and 5% (see Table S2). The application of this new criterion appears to have significantly improved our ability to measure a known laboratory dose accurately.

If we also apply this additional rejection criterion to the other methods of calculating the mean dose (average and $CAM_{UL}$) then the average dose recovery for the arithmetic mean and the IQR average are both acceptable (1.07±0.05 and 0.95±0.03, respectively), whereas the $CAM_{UL}$ average dose recovery ratio is 0.86±0.03, which is not acceptable.

Thomsen et al. (submitted) and Guérin et al. (2015a) applied the $D_0$ rejection criterion to natural single-grain dose distributions for which the CAM ages underestimated the expected ages based on independent age control and found an improvement in their single-grain ages; it was suggested that this method of analysis reduces a bias towards low doses in the dose distribution by only accepting grains which are able to record the absorbed dose accurately. Since the dose recovery dose distributions of the Tabernas Basin samples suffer from a

problem with the inclusion of grains with low $D_0$ values it is very likely that so will the natural dose distributions. Thus, the effect of this criterion on the natural dose distributions is examined below.

# 6 Dose distributions and OSL ages

A summary of the multi-grain and single grain quartz OSL doses for the five terrace samples and the two modern analogue samples is presented in Table 1 and 3. Because of the CAM log-normal assumption, this model cannot be applied to the dose distributions obtained for the two modern analogue samples (MA1 and MA2) and samples Tab-9 and -20, all of which contain non-positive dose estimates (see Fig. 3). The CAM dose estimates given in Table 1 and 3 for samples Tab-9 and -20 have been derived after the arbitrary rejection of these non-positive dose estimates. The calculation of the arithmetic average, IQR and $CAM_{UL}$ doses does not involve any arbitrary rejection of data.

## 6.1 Modern analogue results

The single-grain dose distributions for the two modern analogue samples are shown in Fig. 3A (MA1) and 3B (MA2). The main reason for undertaking OSL measurement of these samples is to investigate whether it is likely that the fossil samples suffer from significant incomplete bleaching. Both single-grain dose distributions appear to be relatively well-bleached, i.e. the dose distributions appear close to symmetrical with only few “outlying” poorly known dose estimates. If these samples are representative of our fossil deposits then it would clearly be incorrect to employ minimum age models (e.g. MAM, Galbraith et al., 1999) or the finite mixture model (FMM; Galbraith and Green, 1990) to address incomplete bleaching in our older samples. Equally, for these modern analogues it would clearly be incorrect to calculate CAM equivalent dose estimates; rejecting the (legitimate) non-positive dose estimates would lead to a significant bias towards higher doses. The resulting $CAM_{UL}$ single-grain ages are 0.08±0.06 and 0.40±0.14 ka, respectively (see Table 4). Note that the application of the $D_0$ criterion to these young samples does not result in the rejection of any grains and so the dose distributions remain unchanged. This is because the average equivalent doses are small compared to all measured $D_0$ values. The arithmetic average doses are biased by high-dose outliers, but applying the IQR reduces both the average and the variance in the dose distributions; if the IQR is used to reject outliers the $CAM_{UL}$ and average (IQR) ages are consistent with each other.

These modern analogue dose distributions and the resulting ages indicate that incomplete bleaching should not be of significant concern in this environment for samples older than say a few thousand years; this is especially true if we remember that modern

analogue samples such as these are likely to be worst-case scenarios due to their poor preservation potential (Jain et al., 2004a). These results are also consistent with the review of modern analogue data by Murray et al. (2012).

*A priori* we would expect average multi-grain doses to agree with average single-grain doses for well-bleached samples. However, the multi-grain ages for these two samples are 2.1±0.8 (MA1) and 5.0±0.5 ka (MA2) and thus overestimate the single-grain ages considerably. Single-grain analysis of sample MA2 showed that 24% of the detectable (i.e. $\sigma_{Tn}$<30%) grains were in (or above) saturation and thus it is likely that the large discrepancy between the multi-grain and single-grain age for this sample (~4.5 ka) is due to the inclusion of these grains in the multi-grain analysis. The reason why these grains have sensitivity-corrected natural signals in saturation is beyond the scope of this paper, but it is possible that this is a result of the failure of our SAR protocol with these grains. It is interesting to note that similar findings have been reported by Jain et al. (2004b) and Arnold et al. (2012) in their comparisons of single- and multi-grain data.

## 6.2 Terrace samples

The single-grain dose distributions for the three young samples collected from terrace level 4 (Tab-10, Tab-20 and Tab-21) are shown in Fig. 3C, 3D and 3E. Although, the OD values are high (>60%) these distributions also appear to be relatively well-bleached with only a few outliers at high doses (with the possible exception of Tab-21). This was expected from our modern analogues distributions and suggests that minimum age modelling would be inappropriate. In addition, one single-grain dose distribution (Tab-20) contains negative dose estimates which would have to be arbitrarily discarded in order to allow the application of MAM or FMM because these involve log transforms. The high dose outliers have no significant impact on the weighted dose estimates (CAM and $CAM_{UL}$) but do – as expected - affect the arithmetic averages. $CAM_{UL}$ and IQR doses are all consistent with each other for these samples except for sample Tab-20. About 17% of the single-grain dose estimates for sample Tab-20 are non-positive and thus the CAM dose given in Table 1 is expected to be too high.

Again the multi-grain ages overestimate the single-grain ages by at least a factor of 2, with $CAM_{UL}$ estimates of between 0.20±0.05 ka (Tab-20) and 2.1±0.2 ka (Tab-21) compared to multi-grain age estimates of 2.0±0.3 ka and 6.4±0.8 ka, respectively. The discrepancy between the multi-grain and single grain ages is again presumably due to the presence of saturated grains (ranging between 10 and 15% of the detectable grain population). Using the $D_0$ criterion does not change the single-grain ages of these relatively young samples, because all grains have $D_0$ values larger than 10 Gy.

Fig. 3F and 3G show the single-grain dose distributions for the two samples from terrace level 3, both of which have ODs of >60%. The dose distribution for sample Tab-9 contains three non-positive dose estimates and thus we cannot apply the CAM (or MAM and FMM) without arbitrary rejection of these dose estimates. For these samples, between 15 and 26% of the grains giving detectable OSL signals (i.e. $\sigma_{TN}$<30%) were in or above saturation (see Table 1). If we apply the $D_0$ criterion to these samples (see Table 3) the number of grains in saturation is reduced to between 4 and 11%, and the $D_e$ systematically increases by between 1% ($CAM_{UL}$, IQR) and 53% (CAM).

# 7 Discussion

In Table 4 both multi-grain and single-grain ages after application of the $D_0$ rejection criterion are given for samples Tab-9 and Tab-11. Note that the application of the $D_0$ criterion only affects the natural dose distributions of the two older samples from terrace level 3. No matter which single-grain dose estimation method is used the multi-grain ages are systematically larger than then the single-grain ages; we attribute this to the significant number of grains in saturation. Thus, the most reliable estimate of burial age is most likely to be derived from the single-grain measurements, where these grains can be identified and eliminated. The $CAM_{UL}$ dose recovery was not consistent with unity (0.86±0.03, n=3) and so we do not expect these results to be accurate. Although the CAM dose recovery is acceptable (0.97±0.03, n=3), the CAM cannot be applied to either of the modern analogues or two (out of five) of the fossil sample because of the presence of negative doses. Arbitrary rejection of these negative doses would risk biasing any result to larger values. For the three fossil samples where both $CAM_{UL}$ and CAM can be calculated without the arbitrary rejection of non-positive dose estimates, the ratio between the $CAM_{UL}$ to CAM is on average 0.76±0.02 (n=3). The $CAM_{UL}$ measured to given dose ratio in the three single-grain beta dose recovery experiments described above is 0.86±0.03 (after the application of the $D_0$ criterion, see Table S2), implying that using the $CAM_{UL}$ may lead to significant dose underestimation for these samples and doses (i.e. >15 Gy).

The dose recovery for the arithmetic average is satisfactory (1.07±0.05, n=3) but the presence of clear outliers in the natural dose distributions makes us question the reliability of these results. In contrast, the “robust statistics” analysis (Tukey, 1977) is the only approach which provides a satisfactory dose recovery (0.95±0.03, n=3), a non-subjective means of rejecting outliers and can be applied to all samples. Nevertheless, Table 4 summaries the $CAM_{UL}$ ages, the CAM ages after the arbitrary rejection of negative results and the IQR ages (non-subjective rejection of outliers). Not surprisingly, the single-grain arithmetic averages are consistently larger than all other analyses, because of the high dose outliers. The $CAM_{UL}$

data for the older two samples ages at the low end of the range and are dismissed because of their poor dose recovery in this dose range. The CAM result for one of the oldest samples (Tab-9) requires the arbitrary rejection of three non-positive dose estimates and not surprisingly the resulting age is the oldest of all age estimates suggesting the presence of a bias. In contrast the CAM result for sample Tab-11 did not involve the arbitrary rejection of non-positive data. Finally, the IQR ages for the two oldest samples are both ~16 ka and are consistent with the presumably more reliable CAM age (19±2 ka) for sample Tab-11.

Turning to the young samples, although the arithmetic average and CAM tend to give systematically higher ages (with one samples, Tab-20, requiring the rejection of non-postive dose estimates), the $CAM_{UL}$ and the IQR are broadly consistent with each other and clearly indicate deposition through the Mid- to Late-Holocene.

Although this study has been limited by unfavourable luminescence characteristics, the resulting age estimates do add valuable information to the Tabernas Basin stratigraphy. Given terrace level 3 OSL aggradation ages of ~16 ka, it is inferred that deposition of this level was ongoing throughout MIS2; this is consistent with the idea of formation under periods of climatic variability suggested by e.g. Macklin et al. (2002). The suggestion of terrace aggradation during glacial cycles fits well with regional patterns of terrace formation (Santisteban and Schulte, 2007). Age estimations for terrace level 4 indicate terrace aggradation occurred during the Mid-Late Holocene from 2.8±0.3 ka; although the sample sites on these terraces were buried they were not taken immediately above the base of the terrace sediments and so it is likely that the onset of terrace deposition occurred sometime before this. The abandonment of terrace level 3 at less than ~16 ka provides an older limit to the initiation of terrace level 4. The similarity in age estimates from modern analogue and the youngest terrace level 4 age estimates seems to indicate that this terrace has not yet been completely abandoned; it is presumably still overtopped by large flood events. Our limited chronology is not sufficient to support detailed interpretations of landscape forcing mechanisms; however, it does provide a basis for future geomorphological investigation and application of OSL dating methods in the Tabernas Basin (SE Spain).

# 8 Conclusions

Quartz OSL dating has been applied to samples derived from a Quaternary fluvial terrace staircase in the Tabernas basin, SE Spain. Results from single grain dating on modern analogue samples show that signal bleaching is unlikely to be a significant problem for these samples. However, detailed analysis of single grain results shows that measurements from multi-grain aliquots significantly overestimate equivalent doses. This is

attributed mainly to the presence of saturated grains. A single-grain $D_0$ criterion was then applied to data; this criterion is designed to reduce the bias in dose distributions resulting from the use of grains with a small $D_0$ compared to the expected $D_e$. When applied to the dose distributions of the two older samples (Tab-9 and Tab-11) the average ages systematically increase, especially when using the CAM. In summary, although OSL dating was complicated by poor luminescence properties, the findings of this chronological study are broadly consistent with Harvey et al. (2003) and Alexander et al., (2008) supporting climatically driven controls on sedimentation events within the Tabernas Basin.

## REFERENCES


Alexander, R.W., Calvo-Cases, A., Arnau-Roalen, E., Mather, A.E., Lazaro- Suau, R., 2008. Erosion and stabilisation sequences in relation to base level changes in the El Cautivo badlands, SE Spain. *Geomorphology* 100, 83-90.

Arnold, L., Demuro, M., Ruiz, N., 2012. Empirical insights into multi-grain averaging effects from 'pseudo' single-grain OSL measurements. *Radiation Measurements* 47, 652-658

Arnold L.J., Roberts, R.G., Galbraith, R.F., DeLong, S.B., 2009. A revised burial dose estimation procedure for optical dating of young and modern-age sediments. *Quaternary Geochronology* 4, 306–325.

Bailey, R.M., Arnold, L.J., 2006. Statistical modelling of single grain quartz De distributions and an assessment of procedures for estimating burial dose. *Quaternary Science Reviews* 25, 2475–2502.

Banerjee, D., Murray, A.S., Bøtter-Jensen, L., Lang, A., 2001. Equivalent dose estimation using a single aliquot of polymineral fine grains. *Radiation Measurements* 33, 73–94.

Bøtter-Jensen, L., Thomsen, K.J., Jain, M., 2010. Review of optically stimulated luminescence (OSL) instrumental developments for retrospective dosimetry. *Radiation Measurements* 45, 253-257.

Bøtter-Jensen, L., Andersen, C.E., Duller, G.A.T., Murray, A.S., 2003. Developments in radiation, stimulation and observation facilities in luminescence measurements. *Radiation Measurements* 37, 535-541.

Duller, G.A.T., 2008. Single-grain optical dating of Quaternary sediments: why aliquot size matters in luminescence dating. *Boreas* 37, 589–612.

Duller, G.A.T., 2007. Assessing the error on equivalent dose estimates derived from single aliquot regenerative dose measurements. *Ancient TL* 25, 15-24.

Duller, G.A.T., 2003. Distinguishing quartz and feldspar in single grain luminescence measurements. *Radiation Measurements* 37, 161-165.Galbraith R.F., Roberts R.G., Laslett G.M., Yoshida H., Olley J.M., 1999. Optical dating of single and multiple grains of quartz from Jinmium rock shelter, northern Australia: Part I, experimental design and statistical models. *Archaeometry* 41, 339–364.

Galbraith, R.F., Green, P.F., 1990. Estimating the component ages in a finite mixture. *Nuclear Tracks and Radiation Measurements* 17, 197-206.

Geach, M.R., Stokes, M., Telfer, M.W., Mather, A.E., Fyfe, R.M., Lewin, S., 2014. The application of geospatial interpolation methods in the reconstruction of Quaternary landform records. *Geomorphology* 216, 234-246.

Guérin, G., Frouin, M., Talamo, S., Aldeias, V., Bruxelles, L., Chiotti, L., Dibble, H.L., Goldberg, P., Hublin, J-J., Jain, M., Lahaye, C., Madelaine, S., Maureille, B., McPherron, S.P., Mercier, N., Murray, A.S., Sandgathe, D., Steele, T.E., Thomsen, K.J., Turq, A. 2015a. A Multi-method Luminescence Dating of the Palaeolithic Sequence of La Ferrassie Based on New Excavations Adjacent to the La Ferrassie 1 and 2 Skeletons. *Journal of Archaeological Science*. doi:10.1016/j.jas.2015.01.019

Guérin, G., Jain, M., Thomsen, K.J., Murray, A.S., Mercier, N., 2015b. Modelling dose rate to single grains of quartz in well-sorted sand samples: The dispersion arising from the presence of potassium feldspars and implications for single grain OSL dating. *Quaternary Geochronology* 27, 52-65.

Guérin, G., Mercier, N., Adamiec, G., 2011. Dose-rate conversion factors: update. *Ancient TL*, 29, 5-8.

Harvey, A.M., Foster, G., Hannam, J., Mather, A.E., 2003. The Tabernas alluvial fan and lake system, southeast Spain: applications of mineral magnetic and pedogenic iron oxide analyses towards clarifying the Quaternary sediment sequences. *Geomorphology* 50, 151-171.

Jain, M., Murray, A.S., Bøtter-Jensen, L., 2004a. Optically stimulated luminescence dating: how significant is incomplete light exposure in fluvial environments? *Quaternaire*, 143-157

Jain, M., Thomsen, K.J., Bøtter-Jensen, L., Murray, A.S., 2004b. Thermal transfer and apparent-dose distributions in poorly bleached mortar samples: Results from single grains and small aliquots of quartz. *Radiation Measurements* 38, 101-109.

Kristensen, J.A., Thomsen. K.J., Murray, A.S., Buylaert, J.P., Jain, M., Breuning-Madsen, H.. Quantification of termite bioturbation in a savannah ecosystem: application of OSL dating. *Quaternary Geochronology,* http://dx.doi.org/10.1016/j.quageo.2015.02.026.

Macklin, M.G., Fuller, I.C., Lewin. J., Maas, G.S., Passmore, D.G., Rose, J., Woodward, J.C., Black, S., Hamlin, R.H.B., Rowan, J.S., 2002. Correlation of fluvial sequences in the Mediterranean basin over the last 200 ka and their relationship to climate change. *Quaternary Science Review*s 21, 1633-1641.

Medialdea, A., Thomsen, K.J., Murray, A.S., Benito, G., 2014. Reliability of equivalent-dose determination and age-models in the OSL dating of historical and modern palaeoflood sediments. *Quaternary Geochronology* 22, 11-24.

Mejdahl, V., 1987. Internal radioactivity in quartz and feldspar grains. *Ancient TL* 5, 10-17.

Murray, A.S, Thomsen, K.J., Masuda, N., Buylaert, J.P., Jain, M., 2012. Identifying well-bleached quartz using the different bleaching rates of quartz and feldspar luminescence signals. *Radiation Measurements* 47, 688-696.

Murray, A.S. and Olley, J.M., 2002. Precision and accuracy in the optically stimulated luminescence dating of sedimentary quartz: a status review. *Geochronometria* 21, 1-16.

Murray, A.S., Wintle A.G., 2000. Luminescence dating of quartz using an improved single-aliquot regenerative-dose protocol. *Radiation Measurements* 32, 57−73.

Murray A.S., 1996. Developments in optically transferred luminescence and photo-transferred thermoluminescence dating: application to a 2000-year sequence of flood deposits. *Geochimica et Cosmochimica Acta* 60, 565-576.

Murray, A.S., Marten, R., Johnston, A., Martin, P., 1987. Analysis for naturallyoccurring radionuclides at environmental concentrations by gamma spectrometry. *J. Radioanal. Nucl. Chem*. 115, 263-288.

Nash, D.J., Smith, R.F., 2003. Properties and development of channel calcretes in a mountain catchment, Tabernas Basin, southeast Spain. Geomorphology 50, 227-250.

Nogueras, P., Burjachs, F., Gallart, F., Puigdefábregas, J., 2000. Recent gully erosion in the El Cautivo badlands (Tabernas, SE Spain). *Catena* 40, 203-215.

Olley, J.M., Caitcheon, G.G., Roberts, R.G., 1999. The origin of dose distributions in fluvial sediments, and the prospect of dating single grains from fluvial deposits using optically stimulated luminescence. *Radiation Measurements* 30, 207-217.

Porat, N., Amit, R., Enzel, Y., Zilberman, E., Avni, Y., Ginat, H., Gluck, D., 2010. Abandonment ages of alluvial landforms in the hyperarid Negev determined by luminescence dating. *Journal of Arid Environments* 74, 861-869.

Roberts, R.G., Galbraith, R.F., Yoshida, H., Laslett, G.M., Olley, J.M., 2000. Distinguishing dose populations in sediment mixtures: a test of single-grain optical dating procedures using mixtures of laboratory-dosed quartz. *Radiation Measurements* 32, 459-465.

Prescott, J.R., Hutton, J.T., 1995. Environmental dose rates and radioactive disequilibrium from some Australian luminescence dating sites. *Quaternary Science Reviews* 14, 439-448.

Santisteban, J.I., Schulte, L., 2007. Fluvial networks of the Iberian Peninsula: a chronological framework. *Quaternary Science Reviews* 26, 2738-2757.

Thomsen, K.J., Murray, A.S., Buylaert, J.P., Jain, M., Hansen, J.H., Aubry,T., In review. Testing single-grain quartz OSL methods using known age samples from the Bordes-Fitte rockshelter (Roches d'Abilly site, Central France). *Quaternary Geochronology.*

Thomsen, K.J., Kook, M., Murray, A.S., Jain, M., Lapp, T., 2015. Single-grain results from an EMCCD-based imaging system, Radiation Measurements, http://dx.doi.org/10.1016/j.radmeas.2015.02.015.

Thomsen, K.J., Murray, A.S., Jain, M., 2012. The dose dependency of the over-dispersion of quartz OSL single grain dose distributions. *Radiation Measurements* 47, 732-739.

Tukey, J.W., 1977. Exploratory Data Analysis. Addison Wesley, Reading, Mass.

Vandenberghe, D., Derese, C., Houbrechts, G., 2007. Residual doses in recent alluvial sediments from the Ardenne (S Belgium). *Geochronometria* 28, 1-8.

Wallinga, J., 2002. Detection of OSL age overestimation using single-aliquot techniques. *Geochronometria* 21, 17–20.

## FIGURE CAPTIONS

Figure 1: (A) Terrace map for the Tabernas Basin. (B) Schematic cross section of terrace staircase detailing sedimentology and incision depths to current drainages. Digital data sourced from: Centro Nacional de Información Geográfica (CNIG, 2013).

Figure 2: Multi-grain OSL characteristics. (A) Preheat plateau for sample Tab-11. (B) Typical quartz OSL dose response curve for sample Tab-9. Inset shows a typical natural decay curve. (C) Histogram of dose recovery ratios (i.e. measured dose divided by given dose) for individual aliquots. The inset shows average dose recovery ratios as a function of given dose. The given dose was chosen to match the measured natural dose.

Figure 3: Natural single-grain quartz dose distributions for A), B) the two modern analogues (MA1 and MA2) and C), D), E), F) and G) the five terrace samples (Tab-9, -10,-11,-20,-21).

**Figures all**

Figure 1

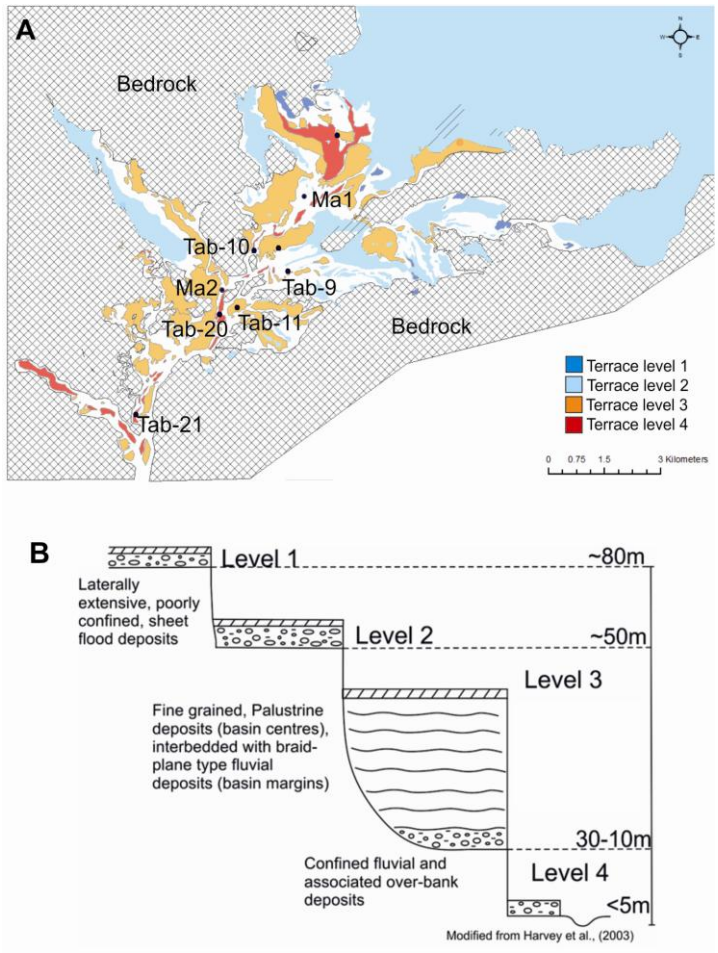

Figure 2

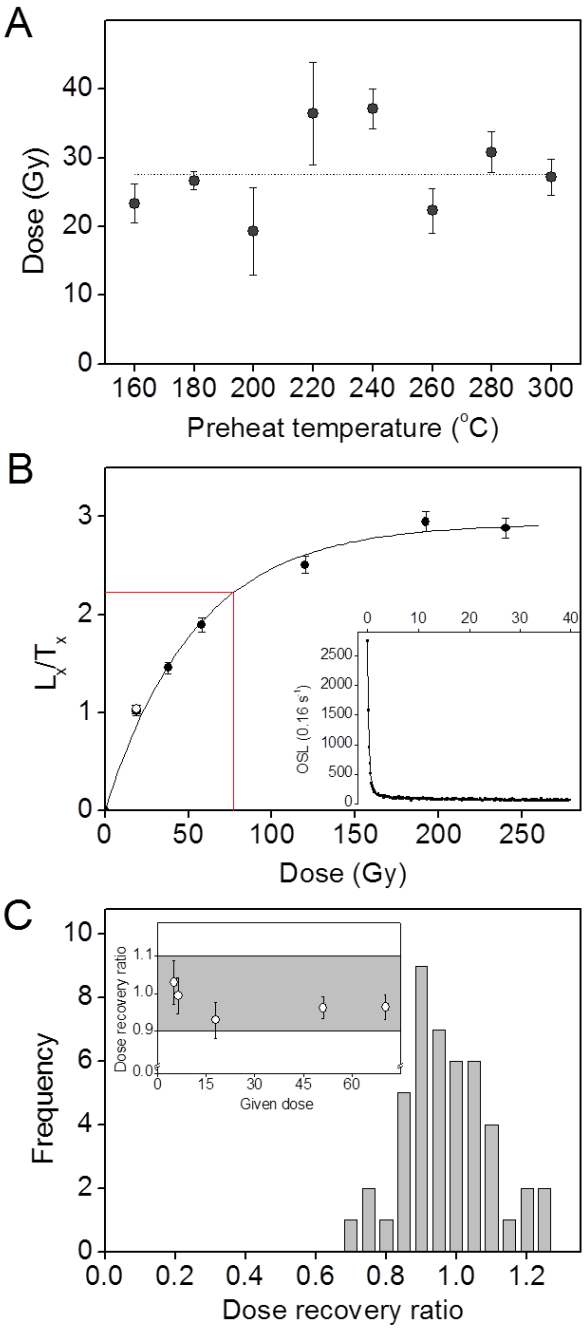
A
Dose (Gy)
0
10
20
30
40
160 180 200 220 240 260 280 300
Preheat temperature (°C)
B
$L_x/T_x$
0
1
2
3
0 50 100 150 200 250
Dose (Gy)
0 10 20 30 40
OSL (0.16 s⁻¹)
0
500
1000
1500
2000
2500
C
Frequency
0
2
4
6
8
10
0.0 0.2 0.4 0.6 0.8 1.0 1.2
Dose recovery ratio
Dose recovery ratio
0.0
0.9
1.0
1.1
0 15 30 45 60
Given dose

Figure 3

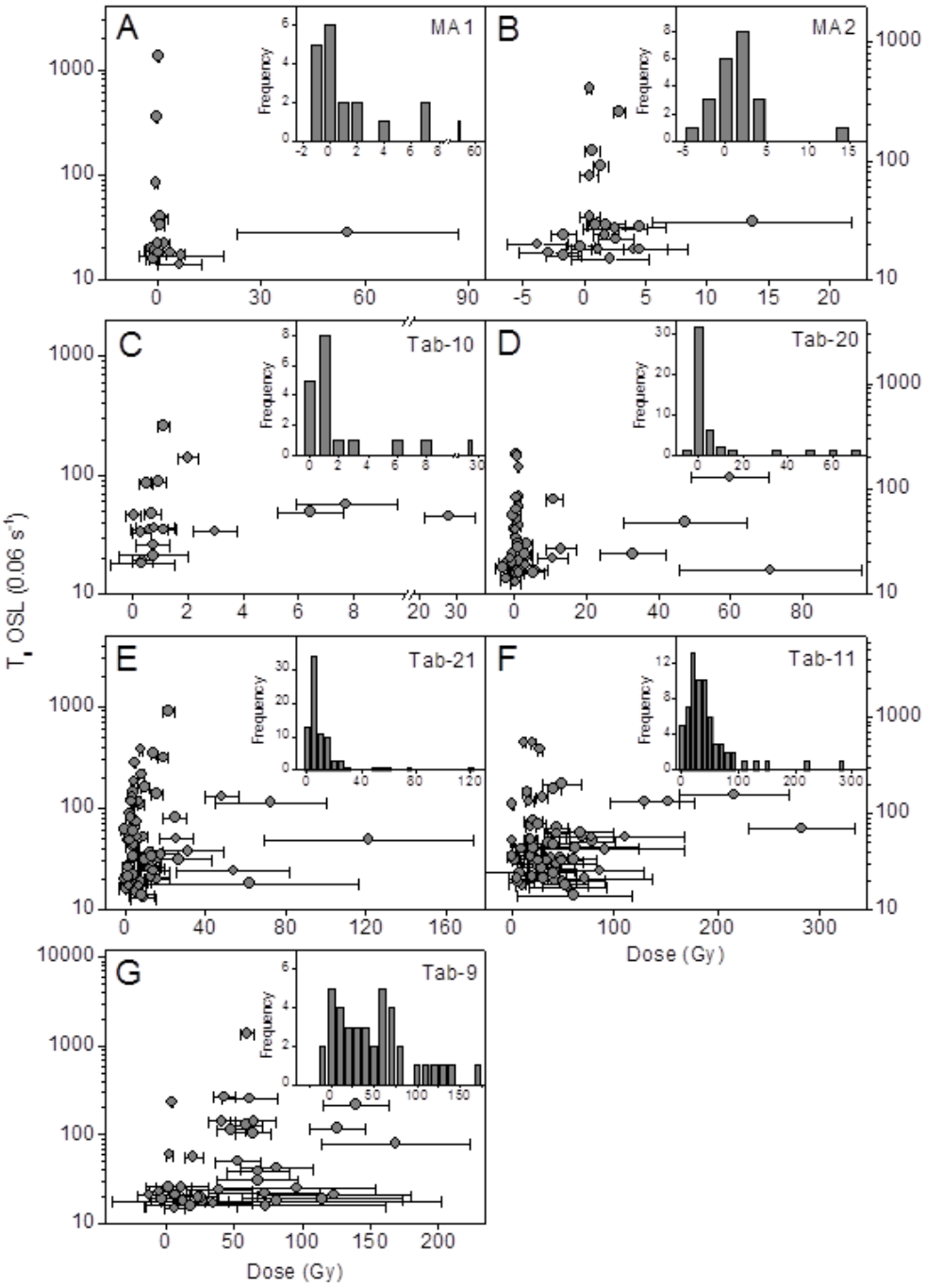
A
MA1
B
MA2
C
Tab-10
D
Tab-20
E
Tab-21
F
Tab-11
G
Tab-9
Frequency
T, OSL (0.06 s⁻¹)
Dose (Gy)

**Tables all**

Table 1. Summary of quartz multi-grain and single-grain results

| Sample | Terrace Level | Single-grain (SG) | | | | | | | | | | | Multi-grain (MG) | |
|---|---|---|---|---|---|---|---|---|---|---|---|---|---|---|
| | | N | $n_{SAT}$ | $n_{SAT}$ (%) | n | Av. (Gy) | CAM (Gy) | OD (%) | $CAM_{UL}$ (Gy) | $OD_{UL}$ (%) | $n_{IQR}$ | IQR (Gy) | Av. (Gy) | n |
| Tab-9 | 3 | 3000 | 14 | 26% | 39 | 49 ± 7 | *47 ± 8* | *77 ± 12* | 38 ± 6 | 80 ± 19 | 29 | 38 ± 5 | 71 ± 3 | 18 |
| Tab-11 | 3 | 4000 | 12 | 15% | 66 | 45 ± 6 | 33 ± 4 | 81 ± 10 | 27 ± 3 | 62 ± 15 | 41 | 31 ± 2 | 51 ± 2 | 31 |
| Tab-10 | 4 | 4600 | 2 | 10% | 18 | 3 ± 2 | 1.6 ± 0.5 | 113 ± 23 | 1.2 ± 0.3 | 83 ± 50 | 12 | 0.69 ± 0.08 | 5.4 ± 0.4 | 41 |
| Tab-20 | 4 | 2400 | 5 | 10% | 46 | 6 ± 2 | *2.6 ± 0.7* | *143 ± 20* | 0.6 ± 0.2 | 70 ± 44 | 29 | 1.2 ± 0.2 | 6.1 ± 0.8 | 18 |
| Tab-21 | 4 | 2400 | 14 | 15% | 80 | 12 ± 2 | 7.7 ± 0.8 | 80 ± 9 | 6.0 ± 0.6 | 64 ± 13 | 63 | 5.7 ± 0.5 | 18 ± 2 | 19 |
| MA1 | Modern | 2400 | 1 | 5% | 19 | 4 ± 3 | n/a | n/a | 0.19 ± 0.13 | - | 15 | 0.0 ± 0.3 | 5 ± 2 | 10 |
| MA2 | Modern | 2400 | 7 | 24% | 22 | 1.6 ± 0.7 | n/a | n/a | 0.9 ± 0.3 | 94 ± 48 | 14 | 1.4 ± 0.3 | 12 ± 1 | 12 |

Note: N is total number of measured single-grains and n is the number of aliquots accepted into the dose distributions. $n_{SAT}$ is the relative number of grains discarded due to saturation. The average dose (Av.) is the unweighted arithmetic dose. The CAM doses for Tab-9 and Tab-20 have been calculated after the arbitary rejection of three and eight non-positive dose estimates, respectively.

Table 2. Summary of dosimetric information for the dated samples.

| Sample | depth (cm) | w.c. (%) | $^{238}U$ ($Bq.kg^{-1}$) | $^{226}Ra$ ($Bq.kg^{-1}$) | $^{232}Th$ ($Bq.kg^{-1}$) | $^{40}K$ ($Bq.kg^{-1}$) | Total dose rate ($Gy.ka^{-1}$) |
|---|---|---|---|---|---|---|---|
| Tab-9 | 340 | 12 | 63 ± 19 | 26 ± 1.3 | 35.2 ± 1.3 | 367 ± 20 | 2.35 ± 0.12 |
| Tab-11 | 560 | 8 | 28 ± 7 | 28 ± 0.6 | 25.7 ± 0.6 | 347 ± 9 | 2.03 ± 0.09 |
| Tab-10 | 140 | 8 | 46 ± 16 | 39 ± 1.4 | 48.3 ± 1.4 | 486 ± 22 | 3.05 ± 0.15 |
| Tab-20 | 110 | 10 | 52 ± 14 | 43 ± 1.1 | 48.5 ± 1.0 | 472 ± 17 | 3.06 ± 0.14 |
| Tab-21 | 395 | 5 | 41 ± 8 | 39 ± 0.8 | 48.6 ± 0.9 | 403 ± 11 | 2.81 ± 0.13 |
| MA1 | 10 | 8 | 34 ± 16 | 30 ± 1.2 | 35.6 ± 1.3 | 293 ± 15 | 2.27 ± 0.11 |
| MA2 | 10 | 8 | 32 ± 14 | 32 ± 1.1 | 37.0 ± 1.0 | 355 ± 16 | 2.36 ± 0.11 |

Note: Summary of depth, water content (w.c.), radionuclide concentrations and quartz dose rates. Average life-time burial water content is taken as 20% of the measured saturated water content and an uncertainty of ±4% has been assumed. An internal quartz dose rate of 0.06±0.03 mGy $a^{-1}$ has been assumed (Mejdahl,1987). Total dose rate include cosmic rays and effect of water content.

Table 3. Summary of quartz single-grain results after the application of the $D_0$ criterion

| Sample | Terrace Level | Av. | | | | CAM | | | | | $CAM_{UL}$ | | | | | IQR | | | | |
|---|---|---|---|---|---|---|---|---|---|---|---|---|---|---|---|---|---|---|---|---|
| | | *x* | $n_{SAT,D0}$ (%) | $n_{D0}$ | $D_e$ (Gy) | *x* | $n_{SAT,D0}$ (%) | $n_{D0}$ | $D_e$ (Gy) | OD (%) | *x* | $n_{SAT,D0}$ (%) | $n_{D0}$ | $D_e$ (Gy) | | OD (%) | *x* | $n_{SAT,D0}$ (%) | $n_{D0}$ | $D_e$ (Gy) | |
| Tab-9 | 3 | 50 | 9% | 30 | 53 ± 9 | 70 | 8% | 24 | *72 ± 11* | *46 ± 13* | 40 | 11% | 33 | 41 | ± 7 | 84 ± 21 | 40 | 11% | 25 | 39 | ± 6 |
| Tab-11 | 3 | 50 | 4% | 47 | 53 ± 8 | 40 | 7% | 55 | 38 ± 4 | 70 ± 9 | 25 | 10% | 65 | 28 | ± 3 | 60 ± 17 | 30 | 10% | 41 | 32 | ± 2 |

Note: *x* is the $D_0$ threshold value, $n_{SAT,D0}$ is the relative number of grain discarded due to saturation after the application of the $D_0$ criterion, $n_{D0}$ is the number of aliquots accepted into the dose distributions. Av. is arithmetic average dose. The CAM values for Tab-9 has been calculated after the arbritary rejection of three non-positive dose estimates. Note that the values of $n_{D0}$ under IQR include the effect of the application of the IQR as well as the application of the $D_0$ criterion. Application of the D0 criterion to samples Tab-10,-20,-21, MA1 and MA2 does not lead to the rejection of any grains and the results for those samples are thus identical to the ones given in Table 1.

Table 4. OSL ages

| Sample | Terrace Level | MG age (ka) | SG age (ka) | | | |
|---|---|---|---|---|---|---|
| | | Av. | Av. | CAM | $CAM_{UL}$ | IQR |
| Tab-9 | 3 | 30 ± 2 | 22 ± 4 | *31 ± 5* | 17 ± 3 | 17 ± 3 |
| Tab-11 | 3 | 25 ± 2 | 26 ± 4 | 19 ± 2 | 14 ± 2 | 15.6 ± 1.2 |
| Tab-10 | 4 | 1.8 ± 0.2 | 1.0 ± 0.5 | 0.5 ± 0.2 | 0.40 ± 0.11 | 0.23 ± 0.03 |
| Tab-20 | 4 | 2.0 ± 0.3 | 2.0 ± 0.8 | *0.8 ± 0.2* | 0.20 ± 0.05 | 0.38 ± 0.06 |
| Tab-21 | 4 | 6.4 ± 0.8 | 4.2 ± 0.8 | 2.7 ± 0.3 | 2.1 ± 0.2 | 2.0 ± 0.2 |
| MA1 | Modern | 2.1 ± 0.8 | 1.7 ± 1.3 | | 0.08 ± 0.06 | 0.01 ± 0.12 |
| MA2 | Modern | 5.0 ± 0.5 | 0.7 ± 0.3 | | 0.40 ± 0.14 | 0.57 ± 0.11 |

Note: Multi-grain (MG) ages are based on arithmetic dose averages (Av.), whereas single-grain (SG) ages are based on arithmetic dose averages (Av.), CAM, $CAM_{UL}$ and unweighted dose averages after the arbitrary but non-subjective rejection of outliers. The single-grain ages for Tab-9 and Tab-11 are based on the dose distributions obtained after application of the $D_0$ criterion. The uncertainties assigned to the ages include a contribution of 2% to allow for uncertainties in the dose rate of the laboratory beta sources. The CAM ages for samples Tab-9 and Tab-20 have been calculated after the arbitary rejection of non-positive dose estimates.

**Supplementary Data**

**Click here to download Supplementary Data: Supplimentary data ReQUAGEO-D-14-00094.docx**